prion propagation. The lysate of 5V-H19 [*PSI*$^+$] strain was fractionated by centrifugation through a sucrose density gradient (*21*), and Sup35p from various fractions was tested for conversion activity by addition to [*psi*$^-$] lysate containing Sup35NMp and Sup35p. The cytosolic and 100*S* fractions did not cause aggregation of Sup35NMp, but all fractions of greater density—that is, 200*S*, 270*S*, and pellet—contained the conversion activity (Fig. 5). Thus, the converting agent is not the Sup35p^{PSI+} monomer; rather, it appears to be Sup35p^{PSI+} aggregates. These results are compatible with the nucleation model for the Sup35p prion-like conversion. The absence of converting activity in the soluble fraction also suggests that the converting agent is not a cytosolic enzyme that modifies Sup35p. Purification of Sup35Sp^{PSI+} to apparent homogeneity (*22*) showed that the converting activity copurified with Sup35p aggregates (Fig. 5). This confirms the basic assumption of the prion model for [*PSI*$^+$], that the converting agent is an altered form of Sup35p.

The above data allow us to explain the results of in vitro studies of the [*PSI*$^+$] phenomenon. Lysates of [*PSI*$^+$] strains produce nonsense codon readthrough in a cell-free translational reaction, whereas lysates of [*psi*$^-$] strains do not. Mixing of these lysates shows that the [*psi*$^-$] lysate is dominant, and prevents readthrough (*23*). This result contrasts with the dominance of [*PSI*$^+$] over [*psi*$^-$] in vivo. However, our results suggest that the soluble fraction of [*PSI*$^+$] lysates obtained by centrifugation at 100,000*g* that was used for cell-free translation reactions does not have the converting activity.

Our results demonstrate the general similarity of yeast and mammalian prions and provide a support for the "protein only" hypothesis for the inheritance of yeast [*PSI*$^+$] phenotype. However, conversion of yeast Sup35p proceeds much more efficiently than that of mammalian PrP. The in vitro conversion of PrP^C to PrP^{Sc} requires more than 50-fold excess of PrP^{Sc} over PrP^C and incubation of mixed PrP^C and PrP^{Sc} for at least 2 days (*3*). These differences may be quantitative rather than qualitative and may be related to the in vivo properties of these prions. Yeast are rapidly dividing unicellular organisms, and the stable inheritance of [*PSI*$^+$] requires that the time of its replication be less than that of a cell generation, that is, less than 2 hours during an exponential phase of growth. There is no such restriction for nondividing cells of brain tissues, in which the PrP^{Sc} accumulation requires months (*1*).

REFERENCES AND NOTES

1. S. B. Prusiner, *Science* **252**, 1515 (1991); *Annu. Rev. Microbiol*. **48**, 655 (1994).
2. J. S. Griffith, *Nature* **215**, 1043 (1967).
3. D. A. Kocisko *et al*., *ibid.* **370**, 471 (1994).
4. B. S. Cox, *Heredity* **20**, 505 (1965); M. Aigle and F. Lacroute, *Mol. Gen. Genet.* **136**, 327 (1975).
5. R. B. Wickner, *Science* **264**, 566 (1994).
6. S. V. Paushkin *et al*., *EMBO J*. **15**, 3127 (1996).
7. M. M. Patino, J.-J. Liu, J. R. Glover, S. Lindquist, *Science* **273**, 622 (1996).
8. G. Zhouravleva *et al*., *EMBO J*. **14**, 4065 (1996); L. Frolova *et al.*, *RNA* **2**, 334 (1996).
9. V. V. Kushnirov *et al*., *Gene* **66**, 45 (1988).
10. M. D. Ter-Avanesyan *et al*., *Mol. Microbiol*. **7**, 683 (1993).
11. M. D. Ter-Avanesyan, A. R. Dagkesamanskaya, V. V. Kushnirov, V. N. Smirnov, *Genetics* **137**, 671 (1994).
12. S. V. Paushkin, V. V. Kushnirov, V. N. Smirnov, M. D. Ter-Avanesyan, *Mol. Cell. Biol.* **17**, 2798 (1997).
13. For preparation of cell lysates, yeast cultures were grown in liquid complete medium (YPD) or in medium selective for plasmid markers in the case of transformants to an absorbance at 600 nm of 1.5, collected, washed in water, and lysed by mixing with glass beads in buffer A [25 mM tris-HCl (pH 7.5), 50 mM KCl, 10 mM $MgCl_2$, 1 mM EDTA, 5% glycerol] containing 1 mM phenylmethylsulfonyl fluoride and protease inhibitor mixture as described [*Short Protocols in Molecular Biology*, F. M. Ausubel *et al*., Eds. (Wiley, New York, 1992)]. Cell debris was removed by centrifugation at 15,000*g* for 20 min.
14. S. V. Paushkin, unpublished data .
15. Lysates were prepared as described (*13*), but without addition of protease inhibitors. Each reaction contained 150 μg of total protein and proteinase K (0.4 to 4.0 μg/ml) (Boehringer Mannheim) in a volume of 50 μl. After a 30-min incubation at 37°C, portions (4 μl) were removed and analyzed by protein immunoblotting with antibody to Sup35p as described (*6*).
16. The lysates were mixed with the indicated proportion of Sup35p^{PSI+} and Sup35p^{psi-} and after incubation with slow rotation at 4°C, placed on a layer of sucrose (1 ml, 30%) made in buffer A and centrifuged at 200,000*g* for 30 min at 4°C. Resulting fractions were electrophoretically separated, and Sup35p was analyzed by protein immunoblotting as described (*6*). Ribosomes were found mostly in the intermediate sucrose fraction and to a lesser extent in the sedimented material. Sup35p of sucrose fraction of lysate mixes could represent small Sup35p^{PSI+} aggregates or ribosome-bound Sup35p^{psi-} (*6*) or both. Therefore, the extent of conversion reaction was estimated as the Sup35p ratio between cytosolic fraction and sedimented material.
17. F. E. Cohen *et al*., *Science* **264**, 530 (1994).
18. P. Brown, L. G. Goldfarb, D. C. Gajdusek, *Lancet* **337**, 1019 (1991).
19. J. T. Jarrett and P. T. Lansbury, *Cell* **73**, 1055 (1993).
20. B. Caughey, D. A. Kocisko, G. J. Raymond, P. T. Lansbury Jr., *Chem. Biol*. **2**, 807 (1995).
21. The lysate (0.3 ml) of 5V-H19 [*PSI*$^+$] strain was loaded onto a 15 to 40% linear sucrose gradient made in buffer A and centrifuged at 180,000*g* for 3 hours at 4°C. The gradient was fractionated into 0.4-ml portions. The sedimented material was dissolved in a loading volume of buffer A.
22. The lysate of the transformant of 1-5V-H19 [*PSI*$^+$] with Sup35ΔSp-encoding multicopy plasmid (*13*) was treated with ribonuclease A (500 g/ml) for 15 min at 20°C, a high salt concentration (1 M LiCl), and nonionic detergent (1% Triton X-100) for 20 min at 4°C and sedimented by centrifugation through a sucrose layer as described (*16*). The sedimented material was treated again as above, resuspended in buffer A, made either 1.25 M or 2.5 M with GuHCl, incubated for 30 min at 4°C, precipitated by centrifugation through a sucrose layer, and resuspended in buffer A for use in the conversion reaction.
23. M. F. Tuite, B. S. Cox, C. S. McLaughlin, *FEBS Lett*. **225**, 205 (1987).

24. We thank L. Kisselev, M. Tuite, and I. Stansfield for critical reading of the manuscript and K. Jones for antibody to Sup45p. Supported by grants from INTAS and the Russian Foundation for Basic Research to (M.D.T.-A.) and from the Wellcome Trust to (V.V.K.).

1 April 1997; accepted 10 June 1997

Mating Type Switching in Yeast Controlled by Asymmetric Localization of *ASH1* mRNA

Roy M. Long,* Robert H. Singer, Xiuhua Meng, Isabel Gonzalez, Kim Nasmyth, Ralf-Peter Jansen

Cell divisions that produce progeny differing in their patterns of gene expression are key to the development of multicellular organisms. In the budding yeast *Saccharomyces cerevisiae*, mother cells but not daughter cells can switch mating type because they selectively express the *HO* endonuclease gene. This asymmetry is due to the preferential accumulation of an unstable transcriptional repressor protein, Ash1p, in daughter cell nuclei. Here it is shown that *ASH1* messenger RNA (mRNA) preferentially accumulates in daughter cells by a process that is dependent on actin and myosin. A cis-acting element in the 3′-untranslated region of *ASH1* mRNA is sufficient to localize a chimeric RNA to daughter cells. These results suggest that localization of mRNA may have been an early property of the eukaryotic lineage.

During early development, cellular diversity is achieved by differences between cells in their patterns of gene expression. A good example of differential gene expression in lower eukaryotes occurs during the diploidization of homothallic strains of the budding yeast *Saccharomyces cerevisiae* (*1*). Upon germination, haploid spores grow to a critical size and then produce buds. Anaphase takes place at the bud neck, and a complete set of chromosomes is delivered to both the mother cell and the daughter cell (bud). The mother cell can switch its mating type, but the daughter cell cannot. This difference is due to mother cell–specific transcription of the *HO* gene, which encodes an endonuclease that initiates gene conversion at the mating type locus (*2*).

Transcription of *HO* in mother cells is due to the unequal accumulation within

daughter nuclei of a repressor of *HO* transcription called Ash1p (*3*). This accumulation depends on at least five *SHE* genes, one of which (*SHE1*, also known as *MYO4*) encodes a type V myosin (*3*). Because mRNA localization is a common mechanism for generating asymmetric protein distribution in higher eukaryotes (*4*), we investigated the localization of *ASH1* mRNA in the dividing yeast cell.

Using fluorescent in situ hybridization (FISH), we initially analyzed cells carrying the *ASH1* gene on a multicopy plasmid (*5*, *6*). *ASH1* mRNA–specific fluorescence was detected in 7% of the cells from an asynchronous culture. In binucleate cells that had undergone anaphase but not cell separation, *ASH1* mRNA was concentrated at the distal tips of buds. Depending on the genetic background, 35 to 66% of the binucleate cells with a FISH signal showed localization of *ASH1* mRNA. When *ASH1* mRNA was not localized to the bud tip, it often appeared to form filamentous tracks extending from daughter cells into mother cells. In contrast to *ASH1* mRNA, polyadenylated [poly(A)$^+$] RNA was dispersed throughout both mother and daughter cells (Fig. 1A, top row). A null mutant of *ASH1* that had been transformed with the vector control showed no *ASH1* mRNA signal (Fig. 1A, bottom row). Uninucleate unbudded cells also showed *ASH1* mRNA localization in an arc at the periphery on the cell. The unbudded cells most likely reflect cells that have recently finished cytokinesis.

To determine if localization of *ASH1* mRNA to the bud tip resulted in higher rates of Ash1p synthesis in daughter cells, we simultaneously monitored the accumulation of *ASH1* mRNA and Ash1p produced by an epitope-tagged *ASH1* gene integrated at the *ASH1* locus (Fig. 1B). Ash1p accumulated within the daughter nucleus near the *ASH1* mRNA, which appeared to be "tracking" through the bud neck to the tip.

The *she* mutants that do not localize Ash1p asymmetrically (*3*) might do so by mislocalizing *ASH1* mRNA. Analysis of the *she* mutants revealed that *ASH1* mRNA was present in binucleate or unbudded uninucleate cells but that it was no longer asymmetrically distributed (Fig. 2). In *myo4*, *she2*, *she3*, and *she4* mutants, *ASH1* mRNA was commonly distributed in a filamentous-like fashion or in patches at the cell periphery. In contrast, in *she5*/*bni1* mutants, *ASH1* mRNA was mainly concentrated in patches near the bud neck.

The dependence of *ASH1* mRNA localization on the nonessential type V myosin Myo4 suggests that the actin cytoskeleton might participate in the asymmetric accumulation of *ASH1* mRNA and protein. We therefore analyzed the distribution of *ASH1* mRNA and Ash1p in strains carrying mutations that affect actin function. The *act1-133* temperature-sensitive mutation affects the myosin-binding site on actin and prevents bud formation at the restrictive temperature (*7*). In mutant cells growing at the permissive temperature, *ASH1* mRNA was rarely localized to the bud (Fig. 3A), and Ash1p accumulation in binucleate cells was rarely asymmetric (*8*). Although the *ASH1* mRNA was diffusely localized in this mutant, the daughter cell often contained higher amounts of mRNA than the mother cell.

We also investigated the distribution of *ASH1* mRNA and Ash1p in mutants lacking the *TPM1* gene that codes for the major

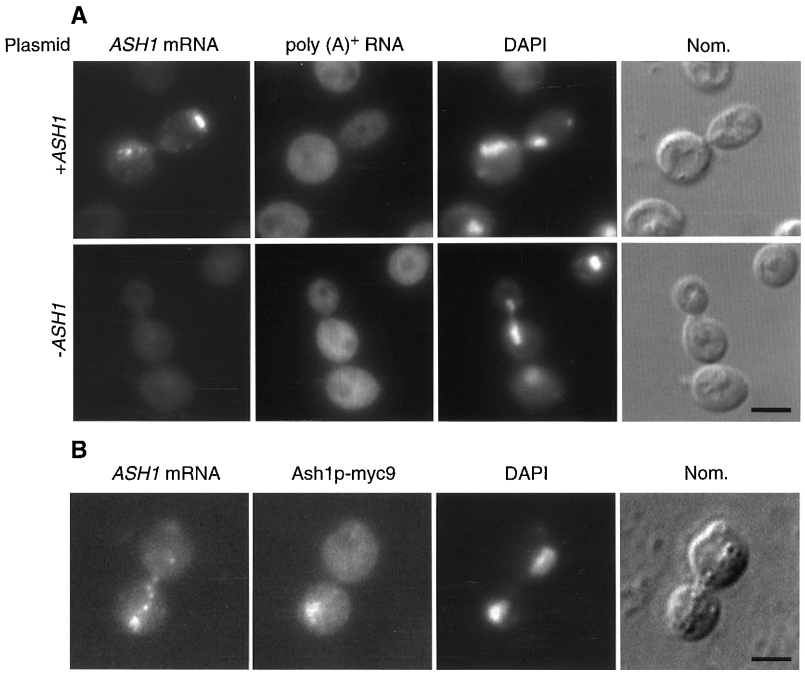

Fig. 1. Localization of *ASH1* mRNA and Ash1p to daughter cells of budding yeast. Bars in Nomarski (Nom.) images in all figures represent 10 μM. (**A**) Simultaneous detection of *ASH1* mRNA and poly(A)$^+$ RNA by FISH (*23*). (**B**) Simultaneous detection of *ASH1* mRNA and Ash1p-myc9 protein (*24*). DAPI, 4′,6′-diamidino-2-phenylindole.

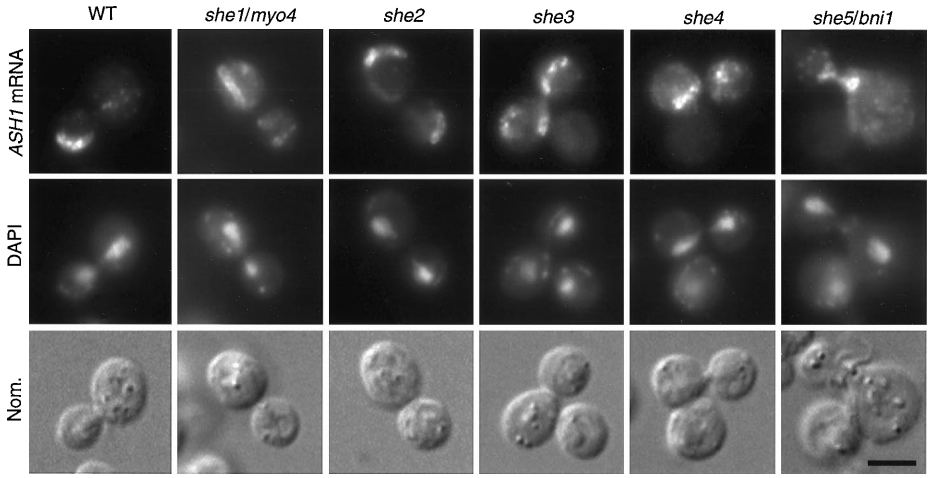

Fig. 2. Dependence of localized *ASH1* mRNA on *SHE1*, *SHE2*, *SHE3*, *SHE4*, and *SHE5*. Fractions of cells with localized *ASH1* mRNA are as follows: K6278 [wild type (WT)], 0.50; K5205 (*she5::URA3*), <0.01; K5209 (*she1::URA3*), 0.01; K5235 (*she3::URA3*), 0.01; K5547 (*she2::URA3*), 0.01; and K5560 (*she4::URA3*), <0.01.

R. M. Long, R. H. Singer, X. Meng, Department of Anatomy and Structural Biology, Albert Einstein College of Medicine, 1300 Morris Park Avenue, Bronx, NY 10461, USA.
I. Gonzalez, K. Nasmyth, R.-P. Jansen, Research Institute of Molecular Pathology, A-1030, Vienna, Austria.

*To whom correspondence should be addressed. E-mail: long@aecom.yu.edu

tropomyosin isotype in yeast or in mutants that are defective in the profilin gene (*PFY1*) (Fig. 3B) (*9*). *ASH1* mRNA was not localized in either mutant but rather had a distribution similar to that observed in the *she1*to *she4* mutants. Ash1p accumulation was rarely asymmetric in binucleate cells (*8*). All three mutants (*act1*, *tpm1*, and *pfy1*) affect the formation of actin cables that run from mother cells into their buds (*7*, *9*).

The defective *ASH1* mRNA and protein localization in these mutants was not an indirect effect of the perturbation in bud formation. Mutants carrying a temperature-sensitive allele of *myo2*, which encodes a type V myosin that is essential for bud formation (*10*), showed asymmetric localization of *ASH1* mRNA and protein at both permissive and restrictive temperatures (Fig. 3C).

To determine if the *ASH1* mRNA at the bud tip was transported through the bud neck and to test whether microtubules are involved in the transport, we analyzed the distribution of *ASH1* mRNA in a *tub2-401* mutant strain, which is defective in the formation of astral microtubules needed for anaphase to take place at the bud neck (*11*). Nuclear division occurs entirely within mother cells when this mutant is shifted to the restrictive temperature (18°C). The *ASH1* mRNA was still localized to the distal bud tip even when nuclear division had occurred within the mother cell (Fig. 4A), indicating that the cells can transport *ASH1* mRNA from the mother cell to the bud tip, despite disruption of microtubules.

The question of whether the *ASH1* mRNA is transported from mother cell nuclei to bud tips was also addressed by experiments in which *ASH1* mRNA was expressed at a stage when there was only a single nucleus. In these experiments, *ASH1* mRNA was expressed from the promoter for the *GAL1* and *GAL10* genes, which is inducible by the addition of galactose to the medium (*12*). The *ASH1* mRNA localized to the bud at all stages of the cell cycle, from the beginning of bud formation during late G_1 to the end of anaphase when *ASH1* mRNA is normally produced; however, no *ASH1* mRNA was detectable when its expression was repressed by glucose (Fig. 4B). This result demonstrates that (i) the mRNA localization mechanism is functional throughout most of the cell cycle; (ii) the mRNAs that are transported to the bud tip include those made within mother cell nuclei; and (iii) the factors at the bud tip that are responsible for attracting or anchoring *ASH1* mRNA are there from the onset of bud formation.

In higher eukaryotic cells, cis-acting sequences that are necessary for mRNA lo-

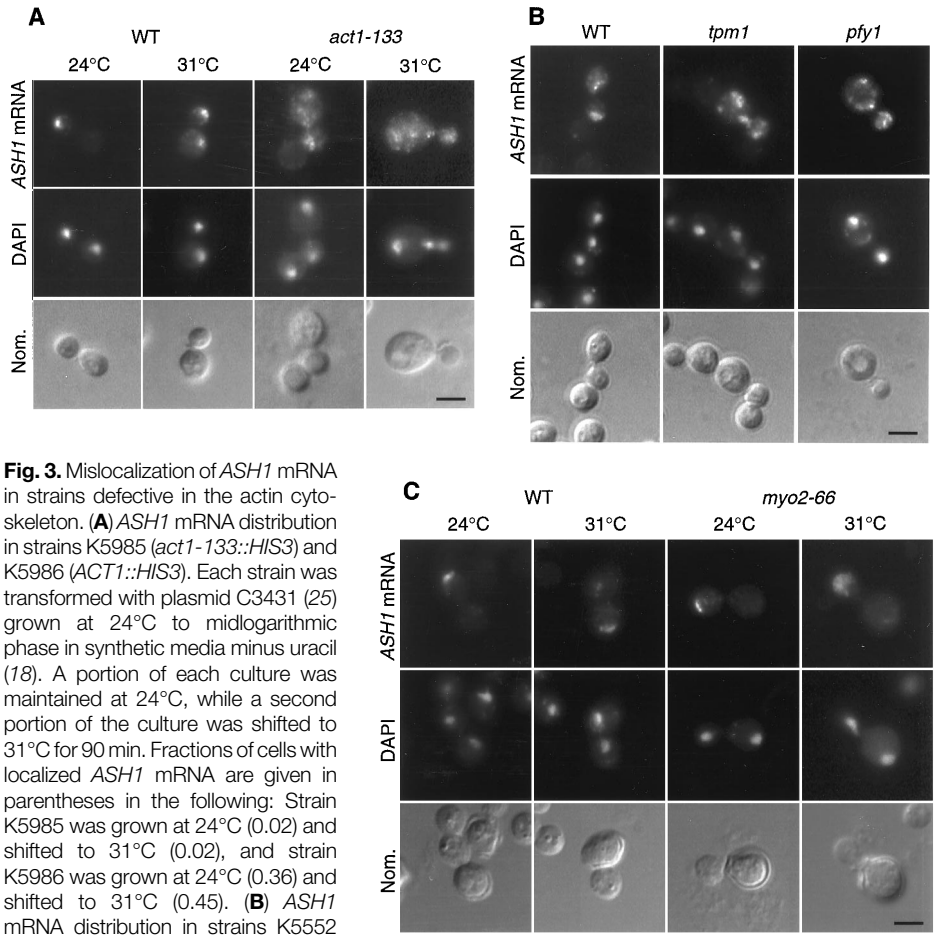

Fig. 3. Mislocalization of *ASH1* mRNA in strains defective in the actin cytoskeleton. (**A**) *ASH1* mRNA distribution in strains K5985 (*act1-133::HIS3*) and K5986 (*ACT1::HIS3*). Each strain was transformed with plasmid C3431 (*25*) grown at 24°C to midlogarithmic phase in synthetic media minus uracil (*18*). A portion of each culture was maintained at 24°C, while a second portion of the culture was shifted to 31°C for 90 min. Fractions of cells with localized *ASH1* mRNA are given in parentheses in the following: Strain K5985 was grown at 24°C (0.02) and shifted to 31°C (0.02), and strain K5986 was grown at 24°C (0.36) and shifted to 31°C (0.45). (**B**) *ASH1* mRNA distribution in strains K5552 (wild type), K5917 (*tpm1Δ::LEU2*), and K5962 (*pfy1-111::LEU2*) (*23*). Each strain was transformed with plasmid C3431 and grown at 24°C. The fractions of cells in each strain with localized *ASH1* mRNA are as follows: K5552, 0.51; K5917, 0.04; and K5962, 0.04. (**C**) *ASH1* mRNA distribution in strains K5552 (wild type) and NY1006 (*myo2-66*) (*10*). Each strain was transformed with plasmid C3319 and grown as described above for the *act1-133* strain.

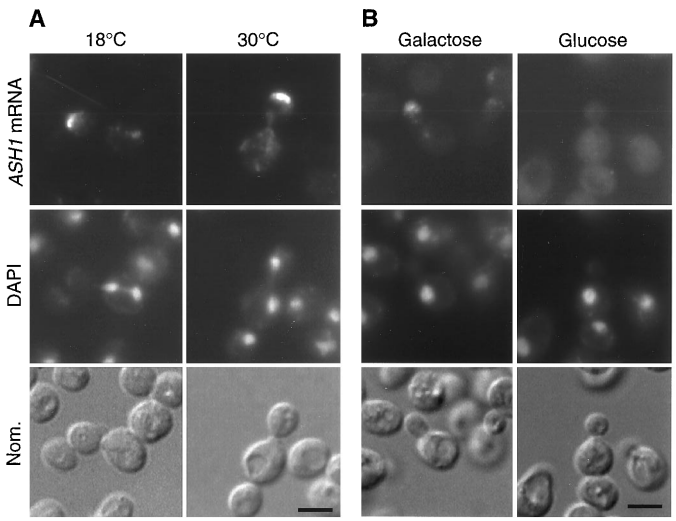

Fig. 4. Transport of *ASH1* mRNA to daughter cells independent of the stage of the cell cycle. (**A**) Localization of *ASH1* mRNA in a *tub2-401* mutant strain determined by FISH. Strain K5429 (*tub2-401*) was transformed with plasmid C3431. Transformants were grown to midlogarithmic phase at the permissive temperature (30°C), and a portion of the culture was shifted to the restrictive temperature (18°C) for 90 min. A second portion of the culture was maintained at 30°C for 90 min. Note at the nonpermissive temperature (18°C) the presence of two nuclei in mother cells, as shown by DAPI staining. (**B**) *ASH1* mRNA localization when expressed from a galactose inducible promoter. Strain K6278 was transformed with plasmid C3348, a derivative of YCplac133 that encodes *ASH1-myc9* under the control of the galactose-inducible promoter *GAL1* (*17*). Transformants were grown to midlogarithmic phase in synthetic liquid media (minus uracil) containing either 2% glucose (repressing conditions) or 3% galactose (inducing conditions).

calization are often confined to the 3′-untranslated region (3′-UTR) of the mRNA (*4, 13*). To address whether *ASH1* mRNA contains a localization signal in its 3′-UTR, a hybrid mRNA was constructed and expressed in yeast. The *Escherichia coli lacZ* coding sequence was fused to 250 nucleotides of *ASH1* 3′-UTR, and the resultant hybrid mRNA expressed from the *GAL1* promoter was detected by FISH. Localization of the hybrid mRNA to the bud in uninucleate small budded cells and to daughters in binucleate budded cells was dependent on the *ASH1* 3′-UTR (Fig. 5) and did not occur when the 3′-UTR from another mRNA (*ADHII*) was substituted (Fig. 5). The localization to buds of the hybrid mRNA containing the *ASH1* 3′-UTR was dependent on *SHE1*, because *she1* mutant cells no longer localize the hybrid mRNA (Fig. 5). Thus, the 3′-UTR of the *ASH1* mRNA appears to contain a cis-acting sequence element that is sufficient to target a heterologous mRNA to the bud. However, the *ASH1* mRNA may contain redundant cis-acting factors that are responsible for *ASH1* mRNA localization, because replacement of the 3′-UTR of *ASH1* with that of *CDC6* only reduced *ASH1* mRNA localization from 56 to 40% and Ash1p asymmetry from 92 to 82%.

The data presented here suggest that localization of *ASH1* mRNA is responsible for the asymmetry in mating type switching through Ash1p. Microscopically, we have shown the juxtaposition of the mRNA in the cytoplasm and the protein in the nucleus (Fig. 1B). Additionally, we have shown that mutations in eight different genes, which cause symmetrical Ash1p accumulation, also abolish localization of *ASH1* mRNA. These observations strongly suggest that *ASH1* mRNA localization is necessary for protein asymmetry. It is unlikely that all these mutations affect independently both mRNA localization and protein asymmetry, especially as some of the mutations (*myo4, she2*, and *she3*) are not very pleiotropic.

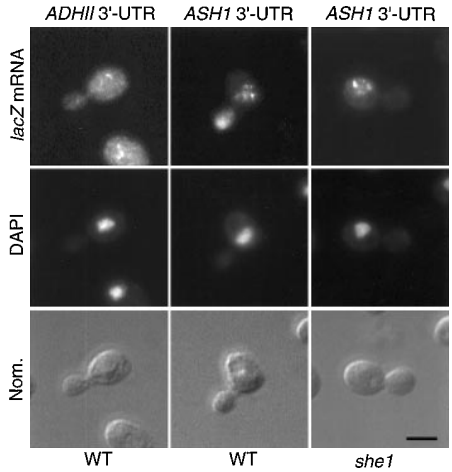

Fig. 5. Localization of a heterologous mRNA to daughter cells through the 3′-UTR of *ASH1*. Strain K6278 was transformed with either plasmid pHZ18-polyadenylate [poly(A)] (*5*) or pXMRS25 (*26*). Plasmid pHZ18-poly(A) contains the *lacZ* reporter gene with the *ADHII* 3′-UTR, whereas pXMRS25 contains the 3′-UTR of *ASH1* in place of *ADHII* sequences. In situ hybridizations to *lacZ* were performed as described previously with the described modifications (*5, 23*).

Cytoplasmic microtubules are thought to have a major role in mRNA localization both in *Drosophila* and *Xenopus* oocytes (*4*). However, actin has been shown to be the filament system that is important for the localization of β-actin mRNA in fibroblasts (*14*). Microtubules are probably not involved in *ASH1* mRNA localization, because disruption of astral microtubules by the *tub2-401* mutation had little or no effect, even though it did prevent nuclei from migrating to the bud neck. Instead, we found that mutations that affect what is presumably an actin-dependent motor protein, Myo4p, as well as mutations in tropomyosin, profilin, and actin itself, all greatly reduce or even abolish *ASH1* mRNA localization to the distal tip. Both profilin and cytoplasmic tropomyosin have been implicated in localizing *oskar* mRNA to the posterior pole of *Drosophila* oocytes (*15*).

We have shown that a mechanism that is capable of moving *ASH1* mRNA to the bud tip exists long before *ASH1* mRNA is actually made in the cell. Possibly, the true cargo for Myo4p is not *ASH1* mRNA itself but some bud tip–specific protein to which *ASH1* mRNA stably binds. Such hypothetical proteins have also been postulated to be the determinants of budding axis in diploid cells (*16*). *ASH1* mRNA, therefore, might not be actively transported at all but merely bound to a receptor, which had previously been delivered to the daughter cell cortex by Myo4p. Irrespective of the actual mechanism by which *ASH1* mRNA is localized, it would seem likely that proteins localized to the distal bud tip act either as addresses or anchors for *ASH1* mRNA. Curiously, none of the proteins currently implicated in *ASH1* mRNA localization are known to be localized at the bud tip at the end of anaphase. This leads us to suspect that as yet unknown components of the localization mechanism await discovery. Likewise, it is probable that other yeast mRNA will be found to be localized to the bud tip or neck.

In multicellular organisms, most localized mRNAs code for proteins involved with differential gene expression. Our data show that asymmetric intracellular mRNA localization is not confined to cells from the animal kingdom or to those from multicellular organisms (*4, 13*). In this light, mRNA localization might be seen as a precursor to, or a substitute for, differential gene expression to generate spatial complexity of proteins.

REFERENCES AND NOTES

1. K. Nasmyth, *Curr. Opin. Genet. Dev.* **3**, 286 (1993).
2. J. N. Strathern and I. Herskowitz, *Cell* **17**, 371 (1979); K. Nasmyth, *Nature* **302**, 670 (1983).
3. N. Bobola, R.-P. Jansen, T. H. Shin, K. Nasmyth, *Cell* **84**, 699 (1996); R.-P. Jansen, C. Dowzer, C. Michaelis, M. Galova, K. Nasmyth, *ibid*., p. 687; A. Sil and I. Herskowitz, *ibid*., p. 711.
4. D. S. Johnson, *ibid*. **81**, 161 (1995); J. Bogucka Glotzer and A. Ephrussi, *Semin. Cell Dev. Biol.* **7**, 357 (1996); O. Steward and R. H. Singer, *mRNA Metabolism and Post-Transcriptional Gene Regulation* (Wiley-Liss, New York, 1997).
5. R. M. Long, D. J. Elliott, F. Stutz, M. Rosbash, R. H. Singer, *RNA* **1**, 1071 (1995).
6. R. M. Long, R.-P. Jansen, I. Gonzalez, K. Nasmyth, R. H. Singer, *Mol. Biol. Cell* **7**, 104a (abstr.) (1996).
7. K. F. Wertman, D. G. Drubin, D. Botstein, *Genetics* **132**, 337 (1992); D. G. Drubin, H. K. Jones, K. F. Wertman, *Mol. Biol. Cell* **4**, 1277 (1993); K. R. Ayscough and D. G. Drubin, *Annu. Rev. Cell Dev. Biol.* **12**, 129 (1996).
8. The fractions of cells showing an asymmetric Ash1p distribution in the various yeast backgrounds are as follows: wild type, 0.95; *myo4*Δ, 0.05; *tpm1*Δ, 0.21; *pfy1-111*, 0.23; *act1-133* at 24°C, 0.12, and at 30°C, 0.07; and *myo2-66* at 24°C, 0.94, and at 30°C, 0.81.
9. H. Liu and A. Bretscher, *Cell* **57**, 233 (1989); B. K. Haarer, A. S. Petzold, S. S. Brown, *Mol. Cell. Biol.* **13**, 7864 (1993).
10. G. C. Johnston, J. A. Prendergast, R. A. Singer, *J. Cell Biol.* **113**, 539 (1991); B. K. Haarer, A. Petzold, S. H. Lillie, S. S. Brown, *J. Cell Sci.* **107**, 1055 (1994); B. Govindan, R. Bowzer, P. Novick, *J. Cell Biol.* **128**, 1055 (1995); K. L. Hill, N. L. Catlett, L. S. Weisman, *ibid*. **135**, 1535 (1996).
11. D. S. Sullivan and T. C. Huffaker, *J. Cell Biol.* **119**, 379 (1992).
12. M. Johnston and R. W. Davis, *Mol. Cell. Biol.* **4**, 1440 (1984).
13. E. H. Kislauskis and R. H. Singer, *Curr. Opin. Cell Biol.* **4**, 975 (1992); R. H. Singer, *Curr. Biol.* **3**, 719 (1993).
14. C. L. Sundell and R. H. Singer, *Science* **253**, 1275 (1991); G. Bassell and R. H. Singer, *Curr. Opin. Cell Biol.* **9**, 109 (1997).
15. M. Erdelyi, A.-M. Michon, A. Guichet, J. Bogucka Glotzer, A. Ephrussi, *Nature* **377**, 524 (1995); L. Manseau, J. Calley, H. Phan, *Development* **122**, 2109 (1996); M. T. Tetzlaff, H. Jaeckle, M. J. Pankratz, *EMBO J.* **15**, 1247 (1996).
16. B. Govindan and P. Novick, *J. Exp. Zool.* **273**, 401 (1995); J. R. Pringle *et al*., *Cold Spring Harbor Symp. Quant. Biol.* **60**, 729 (1995); D. G. Drubin and W. J. Nelson, *Cell* **84**, 335 (1996); T. Roemer, L. G. Vallier, M. Snyder, *Trends Cell Biol.* **6**, 434 (1996).
17. R. D. Gietz and A. Sugino, *Gene* **74**, 527 (1988).
18. F. Sherman, G. R. Fink, J. B. Hicks, *Laboratory Course Manual for Methods in Yeast Genetics* (Cold Spring Harbor Laboratory, Cold Spring Harbor, NY, 1986).
19. K. L. Taneja, M. McCurrach, M. Schalling, D. Housman, R. H. Singer, *J. Cell Biol.* **128**, 995 (1995).
20. J. C. Politz, K. L. Taneja, R. H. Singer, *Nucleic Acids Res.* **23**, 4946 (1995).
21. L. C. Gorsch, T. C. Dockendorff, C. N. Cole, *J. Cell Biol.* **129**, 939 (1995).
22. J. L. Teem and M. Rosbash, *Proc. Natl. Acad. Sci. U.S.A.* **80**, 4403 (1983).
23. Strain 6278 (*ash1::TRP1*) was transformed with plasmid YEplac181 (*17*) and plasmid C3319, a derivative of YEplac181 with a Sal I–Sac I *ASH1* fragment. Transformants were grown in synthetic liquid media (minus leucine) containing 2% glucose until midlogarithmic phase (*18*). *ASH1* mRNA was detected by FISH (*5*) with the following modifications. The amounts of probe and

competitor DNA were reduced from 100 ng and 200 μg to 10 ng and 20 μg, respectively. The composition of buffer B was 1.2 M sorbitol and 10 mM $KHPO_4$ at pH 7.5. After the second posthybridization wash in 40% formamide and 2× standard saline citrate (SSC), a 15-min wash at room temperature in 2× SSC and 0.1% Triton X-100 was done. The oligonucleotide probes were as follows: 5′-GCTT*GCCTTGTTGAATT*CTG-GTGAATT*GCCTGGTGTT*AATGAGGAAATT*GG-3′, 5′-GATGCCTT*AGTGATGGT*AGGCTTTGTTGT*-GGGCGCTCCGGT*CTCTTAGAT*A-3′, 5′-GGA-ACTT*GGACGACCTAGT*CGATTCCAATT*CCTT-GCCGT*AATTGAAACT*AT-3′, 5′-AT*GGTTCTA-TT*GGTTGGTGGACT*CATCGGCGGTGT*GACG-GGAGGAGTAAT*A-3′, 5′-AAGCT*TTGAAACTG-TT*CGTCTTTTTGT*GACTGGCATTT*GGCATGG-GAAAT*G-3′, and 5′-GT*CGAGAGCAAATCTAT*-GATAATTGGG*GACCTTGGGCT*TGGAGTGTAT*-GC-3′. The probes were directly labeled with a Cy3 fluorochrome at amino-modified thymidine residues indicated by the asterisks (*19*). To detect poly(A)$^+$ RNA, FISH was performed with T43 labeled with fluorescein isothiocyanate (*20*). In formamide-containing solutions, the concentration was reduced to 10% for poly(A)$^+$ RNA detection. Images were taken with an Olympus IX70 inverted epifluorescence microscope and Oncor (Gaithersburg, MD) imaging software, version 2.0.5.

24. Strain K5552, which encodes an epitope-tagged version of Ash1p (Ash1p-myc9), was grown to midlogarithmic phase, fixed, and processed for simultaneous FISH and immunofluorescence. After FISH, immunofluorescence was performed as described previously (*21*) with the following alterations. Antibody to myc was diluted 1:5 into a solution of 1× phosphate-buffered saline, 0.1% bovine serum albumin, 20 mM vanadyl ribonucleoside complex, and ribonuclease inhibitor (40 U/μl). The secondary antibody, goat antibody to mouse immunoglobulin G, conjugated to dichlorotrianzinyl amino fluorescein (Jackson Laboratories), was diluted 1:50 into the same solution.
25. Plasmid C3431 is a derivative of YEplac195 (*17*) carrying a Sal I–Sac I ASH1 fragment.
26. Plasmid pHZ18-poly(A) containing the *ADHII* 3′-UTR has been described (*5*). Plasmid pXMRS25 was constructed from pHZ18 (*22*) by insertion of an *ASH1* fragment generated by the polymerase chain reaction (PCR). The PCR product contained the last five amino acid codons of *ASH1* and extended 250 nucleotides beyond the stop codon. The *ASH1* fragment was subcloned into the Sac I site of pHZ18 by the inclusion of a Sac I restriction site in the PCR primers. The primers for PCR were 5′-GGGC-CCGAGCTCGAGACAGTAGAGAATTGATACATG-3′ and 5′-GGGCCCGAGCTCATCAGGATGAC-CAATCTATTGCGC-3′. To verify that no mutations were introduced by PCR, the *ASH1* region of plasmid pXMRS25 was confirmed by DNA sequencing.
27. We thank M. Rosbash for initiating our collaboration and D. Amberg, S. Brown, A. Bretscher, B. Haarer, and P. Novick for providing yeast strains. Supported by NIH grant GM54887 (to R.H.S) and NIH–National Institute of Child Health and Human Development fellowship 7 F32 HD08088-02 (to R.M.L).

17 April 1997; accepted 13 June 1997

TECHNICAL COMMENTS

Genetic Complexity and Parkinson's Disease

Mihael H. Polymeropoulos *et al.* describe the genetic linkage of a large Parkinson's disease (PD) pedigree to chromosome 4q21-q23 (*1*). In this study, which affirms a long hypothesized genetic component to the disease, linkage was detected in a single large family with the use of an autosomal dominant model with 99% penetrance of the disease trait. The clinical presentation in this family, however, may differ from typical idiopathic PD because of the apparent autosomal dominant transmisson, early onset, rapid course, and less frequent occurrence of tremor as a significant sign (*2*). Thus, it is unclear whether the putative PD locus identified by Polymeropoulos *et al.* (which they termed PD1) is responsible for the majority of familial idiopathic PD cases.

As part of an ongoing multicenter study of the genetics of idiopathic PD, we have ascertained 94 Caucasian families (a total of 213 affected relatives sampled: 108 affected sibpairs and 31 affected relative pairs) with at least two individuals in each family meeting clinical criteria for idiopathic PD (*3*). We have identified approximately 200 multiplex idiopathic PD families to ascertain for a genomic screen. The 94 families discussed here were those completely ascertained, with DNA sampled, at the time of the analysis. Linkage analysis of chromosome 4q21-q23 markers in these idiopathic PD families did not reveal evidence for linkage of an autosomal dominant, highly penetrant gene, as was described by Polymeropoulos *et al.* (*1*, *4*). We determined two-point log odds (lod) scores, with the use of the model of Polymeropoulos *et al.* as well as a low penetrance "affecteds-only" autosomal dominant model. These lod scores were strongly negative for markers *D4S2361*, *D4S2409*, *D4S2380*, *D4S1647*, and *D4S2623*. Multipoint analysis of the genetic map *D4S2361-17cM-D4S1647-10.5cM-D4S2623* supported these findings for both models, excluding the entire candidate region. We found no evidence for heterogeneity of either the two-point ($P > 0.20$) or multipoint (ln likelihood = 1) lod scores (*5*). Because the power of the parametric lod score method suffers when the genetic model is misspecified, we also used nonparametric analyses of affected relative pairs (*6*). As with the parametric lod score analysis, we found no significant evidence for linkage using either two-point or multipoint analysis; in this data set, the multipoint location scores (MLS) exclude the entire 27.5 cM region for recurrence risks to siblings as low as 2.5 (Fig. 1). Because the pedigree analyzed by Polymeropoulos *et al.* contained many younger onset cases (mean age at onset of the disease was 46), we repeated our analysis in the 22 families with at least one affected individual with an onset earlier than age 45; the analysis in the subset supported the results from the full sample (*7*).

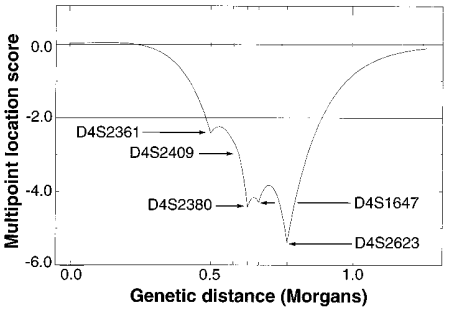

Fig. 1. Multipoint exclusion map for chromosome 4q21-q23 markers. The multipoint lod scores (MLS) within the region are all less than −2.0 at $\lambda_s = 2.5$, excluding the entire candidate region identified by Polymeropoulos *et al.* (*1*). Arrows indicate chromosome markers.

The absence of linkage to chromosome 4q21-q23 in our dataset indicates that there is genetic heterogeneity in PD. It is possible that the region identified by Polymeropoulos *et al.* harbors a disease locus responsible only for a rare autosomal dominant form of PD. Such a situation would be analogous to the genetics of Alzheimer's disease (AD), where mutations (in the amyloid precursor protein and the presenilin 1 and presenilin 2 genes) that cause autosomal dominant AD are responsible for less than 2% of all cases (*8*). Therefore, although the report by Polymeropoulos *et al.* is a first step in unraveling the genetic etiology of PD, other independent genetic effects likely remain to be discovered.

William K. Scott, Jeffrey M. Stajich, Larry H. Yamaoka, Marcy C. Speer, Jeffery M. Vance, Allen D. Roses, Margaret A. Pericak-Vance, and the ***Deane Laboratory Parkinson Disease Research Group*** (*9*), *Department of Medicine, Duke University Medical Center, Durham, NC, 27710, USA; E-mail: mpv@locus.mc.duke.edu*

REFERENCES AND NOTES

1. M. H. Polymeropoulos *et al.*, *Science* **274**, 1197 (1996).
2. L. I. Golbe, G. Di Iorio, V. Bonavita, D. C. Miller, R. C. Duvoisin, *Ann. Neurol.* **27**, 276 (1990).
3. The families enrolled in this study were ascertained in the following manner. Each of the principal investigators of the 12 study sites identified idiopathic PD patients with one or more first-degree relatives with PD. All 94 families included in the analysis were responsive to levodopa. Specifically excluded were patients with a history of encephalitis, neuroleptic therapy within the year before diagnosis, evidence of